LEGIBILITY NOTICE

A major purpose of the Technical Information Center is to provide the broadest dissemination possible of information contained in DOE's Research and Development Reports to business, industry, the academic community, and federal, state and local governments.

Although a small portion of this report is not reproducible, it is being made available to expedite the availability of information on the research discussed herein.

LA-UR -86-3811

Los Alamos National Laboratory is operated by the University of California for the United States Department of Energy under contract W-7405-ENG-36

LA-UR--86-3811

DE87 002914

TITLE MICROSTRUCTURE OF METASTABLE METALLIC ALLOY FILMS PRODUCED BY LASER BREAKDOWN CHEMICAL VAPOR DEPOSITION AND ION IMPLANTATION

AUTHOR(S): Sarath Kumar Menon, MST-5
Thomas Roland Jervis, MST-3
Michael Nastasi, MST-7

Materials Science and Technology Division
Los Alamos National Laboratory
Los Alamos, New Mexico

SUBMITTED TO Proceedings of Material Research Society Symposium on Science and Technology of Rapidly Quenched Alloys, Boston, MA 12/2/86.

DISCLAIMER

MASTER

Los Alamos Los Alamos National Laboratory
Los Alamos, New Mexico 87545

FORM NO 836 R4

MICROSTRUCTURE OF METASTABLE METALLIC ALLOY FILMS PRODUCED BY LASER BREAKDOWN CHEMICAL VAPOR DEPOSITION AND ION IMPLANTATION

S. K. MENON*, T. R. JERVIS, and M. NASTASI
Materials Science and Technology Division, Mailstop E549, Los Alamos National Laboratory, Los Alamos, NM 87545, *Present address: Naval Chemical & Metallurgical Laboratory, Naval Dockyard, Tiger Gate, Bombay 400023, India

ABSTRACT

Thin films produced by laser breakdown chemical vapor deposition from nickel and iron carbonyls and by implanting Ni foils with varying levels of C have been characterized by transmission electron microscopy. Decomposition of $Ni(CO)_4$ produces polycrystalline films of fcc Ni and metastable ordered hexagonal Ni_3C. This metastable phase is identical to that produced by gas carburization, rapid solidification of Ni-C melts, and ion implantation of C into Ni at low concentrations. Increasing the H_2 content in the gas mixture during laser deposition reduces the grain size of the films significantly with grain sizes smaller than 10 nanometers produced. Laser decomposition of $Fe(CO)_5$ produces films with islands of fcc gamma-Fe and finely dispersed metastable Fe_3C (Cementite). In addition, the ferrous oxides Fe_2O_3 and Fe_3O_4 were found in these samples. Implants of C into pure Ni foils at 77°K and at a concentration of 35 at.% produced amorphous layers. Implants at the same dose at room temperature did not produce amorphous layers.

INTRODUCTION

Recently, a new technique for the preparation of thin films by gas phase pyrolysis of metal bearing gas mixtures has been developed[1,2]. The technique utilizes laser dielectric breakdown of gas phase precursors to induce the deposition of metallic films on an unheated substrate. During the process, decomposition and deposition on the substrate occur in a short time (< 2 msec) and hence the entire process is expected to yield non-equilibrium structures. In this work, thin films produced by laser breakdown chemical vapor deposition (LBCVD) from Ni and Fe carbonyls have been examined and their structure characterized with emphasis on identifying the phases present. Comparable structures in the Ni-C system were also produced by ion implantation. In a sample implanted at the highest dose (corresponding to a C concentration of 35 at.%) at 77°K, an amorphous surface layer was formed, indicating that diffusion kinetics limit the formation of the amorphous phase.

EXPERIMENT

Thin films were formed by a laser deposition process in which gas phase chemical reactions are initiated in a flowing gas mixture[2]. Dielectric breakdown in the mixture caused by the focused beam of a pulsed CO_2 laser creates a plasma region a short distance above the substrate. The gas mixture is primarily Ar with at most 3% source gases and up to 50% H_2

when this is a halide. The Ar buffers the reacting species and enhances dielectric breakdown. The substrate is heated only to insure volatility of the source gas ($T < 350$ °K) and there is no direct interaction between the plasma itself and the deposited film so that there is little surface energy available to the depositing materials. This results in direct deposition of metastable forms, even when sufficient rearrangement occurs to form continuous metallic films. For the convenience of microstructural characterization, thin films were deposited on NaCl substrates and the films floated onto 3 mm Cu grids. Implants of C into Ni foils were performed to result in surface layers with C concentrations of 17, 25, and 35 at.%. All specimens were examined in a Phillips 400T transmission electron microscope operating at 120 KV.

RESULTS AND DISCUSSION

Thin films produced by LBCVD from Ni and Fe carbonyls and the surface layers of implanted foils were examined by transmission electron microscopy. The results of the microstructural analysis will be presented and compared in the following sections.

Decomposition of Nickel Carbonyl, $Ni(CO)_4$:

A typical microstructure observed in the LBCVD Ni samples and the corresponding selected area diffraction (SAD) pattern are shown in Fig. 1. As can be seen in Fig. 1(a), the samples produced by LBCVD of $Ni(CO)_4$ are fine-grained (grain size 5-15 nm) polycrystalline films.

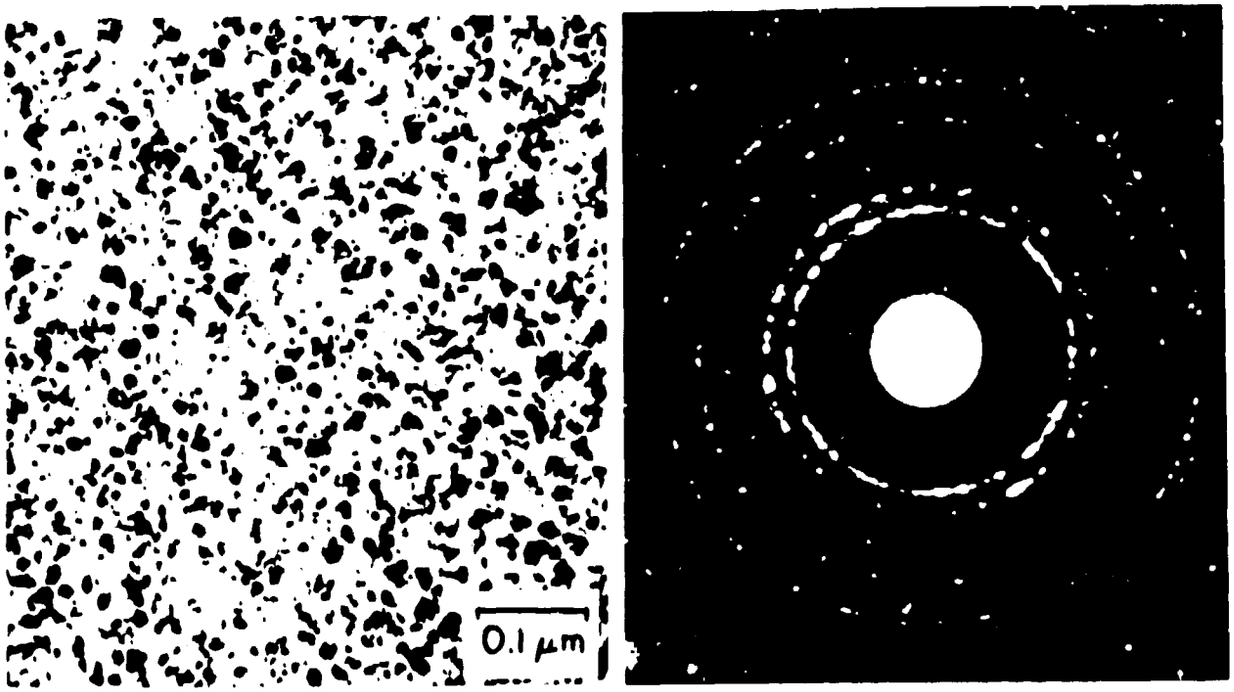

FIG. 1.(a) Brightfield micrograph illustrating the fine grained film deposited by LBCVD from $Ni(CO)_4$. (b) SAD pattern showing the presence of fcc Ni and Ni_3C.

SAD patterns from these samples revealed diffraction spots arranged as nearly continuous rings as shown in Fig 1(b). Analysis of these diffraction patterns revealed that fcc Ni and ordered Ni_3C are present. Table I lists the observed interplanar spacing as measured from the SAD patterns and the indexing scheme. Since the SAD patterns showed many closely spaced rings, often quite weak in intensity, measurement of the d-spacings was aided by microdensitometer traces of the diffraction patterns. The indices for the Ni_3C phase correspond to an ordered hexagonal lattice and matches very well with the structure described by Nagakura[3,4] who obtained this phase by gas carburization of thin Ni films deposited on NaCl crystals. The lattice constants found here are a = 0.455 nm and c = 1.29 nm. This phase has also been obtained in Ni-C alloys by liquid phase quenching[5]. The lattice parameter of the fcc phase was estimated from the electron diffraction data to be 0.359 nm indicating a considerable increase from that of pure Ni (a = 0.35238 nm)[6]. The maximum equilibrium solid solubility of C in Ni is reported to be 2.7 at. %[7-9] and hence it is clear that the LBCVD process leads to a considerable degree of supersaturation in the fcc phase. A rough estimate of the carbon concentration in the fcc phase can be obtained from the relationship a(nm) = 0.35240 + 0.0008 x at. % C as reported by Ruhl and Cohen[10]. Accordingly, the fcc phase produced by LBCVD contains about 7.7 at. % C in solid solution. This is consistent with the metastable equilibrium diagram obtained by Ershova et. al.[9] which indicates a maximum C solubility of 7.4 at.% in the Ni-Ni_3C phase diagram. Auger spectroscopy analysis indicates from 8-25 at.% C in LBCVD films. A very rough estimate based on the lever rule indicates that the samples analysed contain about 14% by volume of the Ni_3C phase. Darkfield microscopy experiments showed that the samples were composed of entire grains of the carbide phase.

TABLE I
Phases Present in Ni Films

Interplanar Spacing (nm)	(h,k,i,l) Ni_3C	(h,k,l) fcc Ni
0.337	$01\bar{1}2$	
0.225	$11\bar{2}0$	
0.212	0006	
0.207		111
0.197	$11\bar{2}3$	
0.179		002
0.155	$11\bar{2}6$	
0.132	$03\bar{3}0$	
0.125	$20\bar{2}8$, $10\bar{1}10$	022
0.120	1129	
0.108	00012	113
0.102	$22\bar{4}6$	222
0.089		004
0.084	$14\bar{5}3$	
0.081		133
0.079	$14\bar{5}6$	

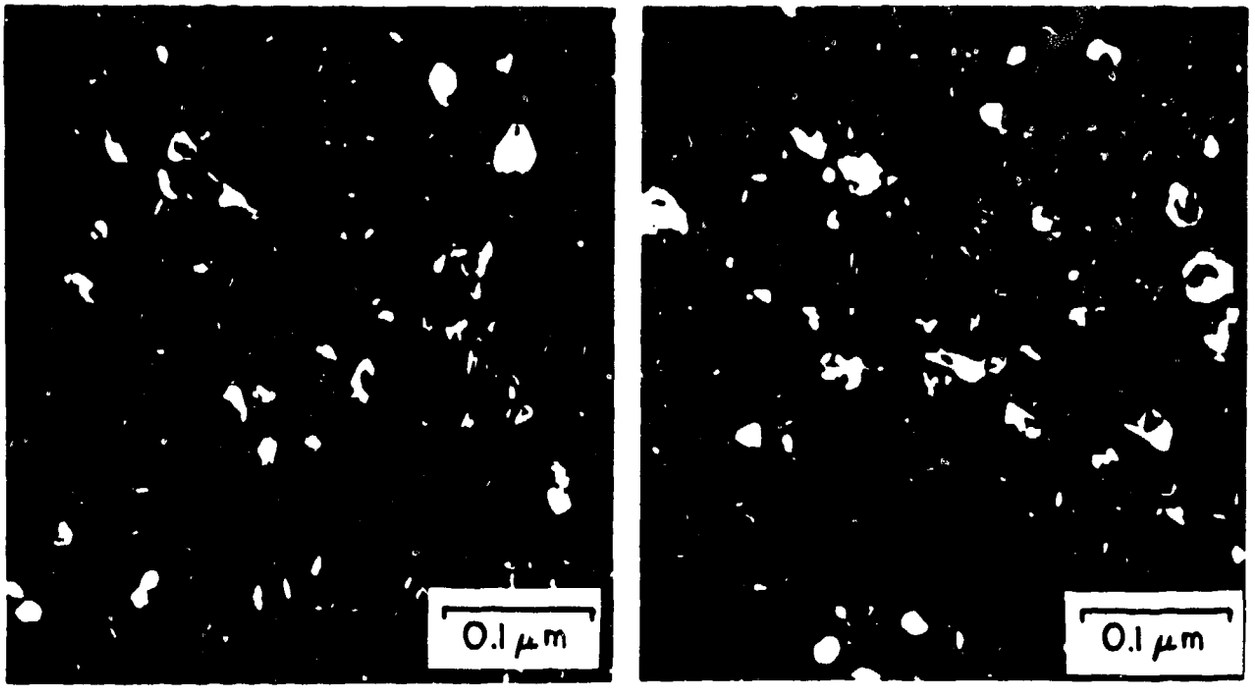

FIGURE 2. Darkfield micrographs of Ni-C film obtained from two positions on the same diffraction ring.

Fig. 2 shows two dark field micrographs from the same area which were obtained by enclosing a large number of diffraction spots within the objective aperture. The two darkfield micrographs shown in Fig 2 were obtained from the same area of the specimen but by positioning the objective aperture at two different positions along the diffraction ring. It is evident from Table I that several d-spacings corresponding to Ni_3C and fcc Ni are very close and one cannot isolate the fcc Ni spots from the Ni_3C spots in the SAD pattern. Dark field micrographs (similar to Fig. 2) obtained from several portions of the diffraction ring failed to show any morphology other than equiaxed grains associated with either of the phases present in the films. Hence, we conclude that both the fcc Ni and Ni_3C grains possess similar equiaxed morphology. These observations suggest that both of these phases nucleated independently from the gas phase rather than forming from a supersaturated fcc solid solution which subsequently precipitated the Ni_3C phase.

Decomposition of iron carbonyl, $Fe(CO)_5$:

Fig. 3 illustrates a typical bright field micrograph and the corresponding SAD pattern obtained from thin films produced by LBCVD of $Fe(CO)_5$. As can be seen from Fig 3(a), the microstructure consists of islands of one phase in a uniform dispersion of very fine precipitates. The structure appears to be much more complex than that of the Ni films. Analysis of the SAD pattern reveals the presence of Fe_2O_3 and Fe_3O_4 in addition to cementite (Fe_3C) and austenite (gamma).

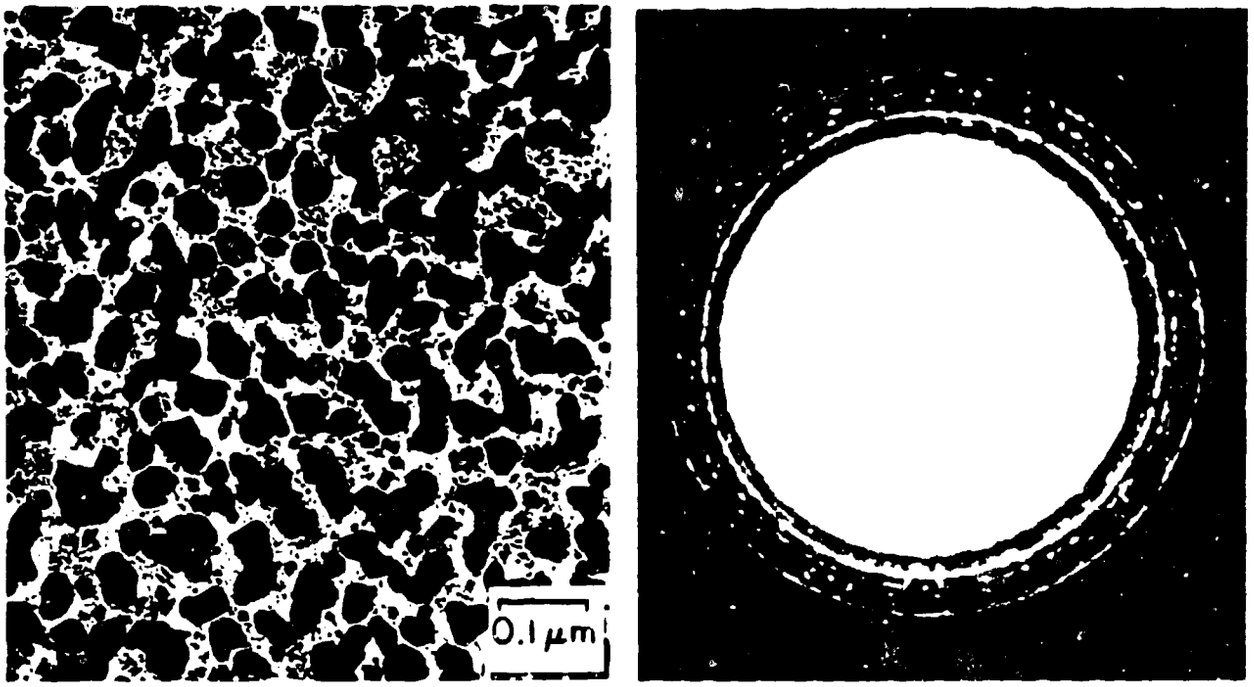

FIGURE 3.(a) Brightfield micrograph illustrating the film produced by LBCVD from $Fe(CO)_5$. (b) SAD pattern showing the presence of multiple phases.

Table II shows a list of the observed d-spacings and the indexing scheme. It appears that both the oxides may simultaneously be present though the analysis is not unambiguous. The interesting point to be noted is that austenite is stabilized and no diffraction spots could be associated with either of the bcc phases of iron. This finding is not really surprising since binary Fe-C austenite can indeed be stabilized at high C concentrations since the martensite start temperature drops to temperatures below room temperature when the carbon content increases beyond 1.23 wt. %[11]. The lattice parameter of the gamma phase estimated from the data in Table II corresponds to 0.365 nm. Based on the lattice parameter vs carbon concentration data reported by Roberts[12], this corresponds to a carbon concentration of 2.32 wt. % (10 at. %) which is slightly higher than the maximum solid solubility of carbon in binary Fe-C austenite reported in the Fe-Fe_3C metastable equilibrium diagram[7].

TABLE II
Phases Present in Fe Films

Interplanar Spacing (nm)	(h,k,l) Fe_2O_3	(h,k,l) Fe_3O_4	(h,k,l) Fe_3C	(h,k,l) gamma
0.251	110	311	020	
0.211			120?	111
0.152		222		
0.129	119	620	312	022
0.125	220	622	140, 313	
0.109	042	731	331	113
0.097	229	751		
0.089	2014	664		

As mentioned before, the microstructure consisted of a distribution of very fine particles of Fe_3C which are best seen in the dark field micrographs shown in Fig. 4. Fig. 4(a) shows a dark field micrograph obtained mainly from the (111)-gamma spots and shows the austenite grains clearly. Fig. 4(b) shows a bimodal distribution of particles with relatively large austenite grains and very fine (5 nm) particles of cementite (Fe_3C). The matrix is presumably a thin film of the oxides.

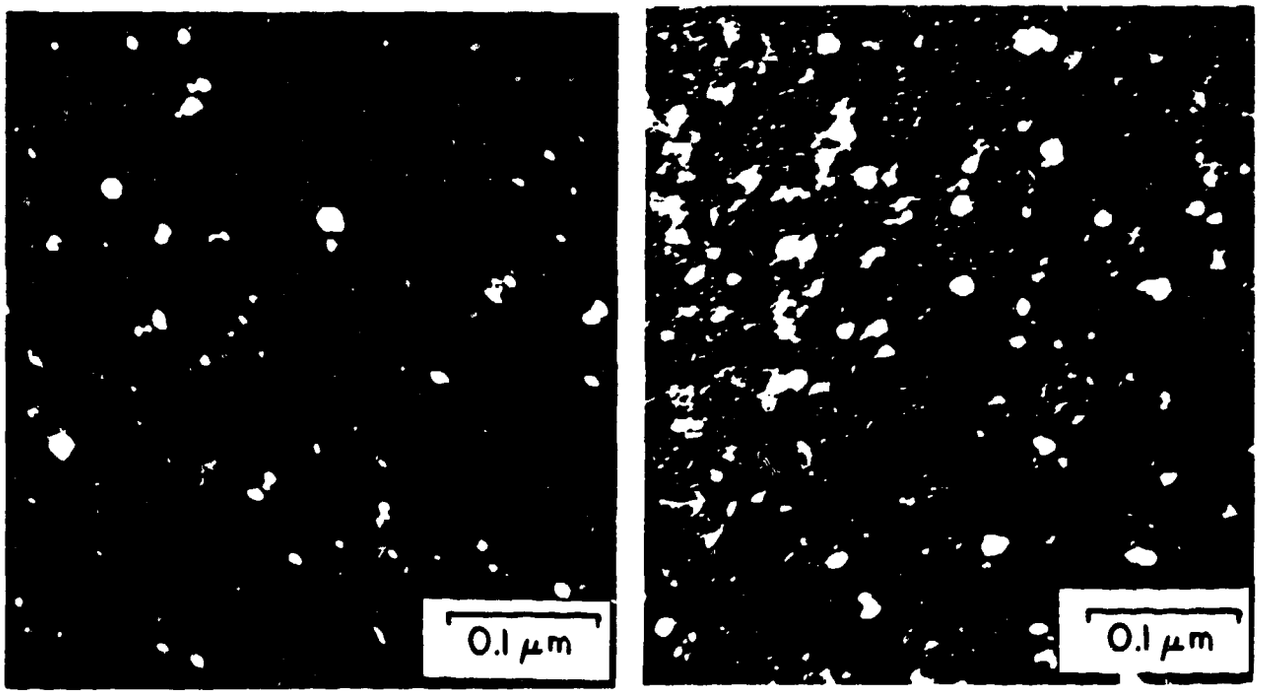

FIGURE 4. Darkfield micrographs of Fe-C film showing size difference between austenite and cementite grains.

Ion Implantation of C into Ni Foils:

Carbon ions were inplanted into pure Ni foils at an energy of 35 KeV, doses of 2.0, 3.0, and 4.2 x 10^{17} /cm^2, and at 2.8 x 10^{-6} A/cm^2. These implants resulted in C concentrations in the surface layer of 17, 25, and 35 at.% as measured by Auger electron spectroscopy. Implants performed at the highest dose were made into substrates held both at room temperature and at 77°K. These foils were subsequently thinned from the back side and ion milled to produce samples for TEM analysis. At concentrations up to 35%, mixed phase microcrystalline Ni and Ni_3C were formed. The Ni_3C microstructure was identical to that found in the LBCVD, liquid quenched, and carburized samples. The microstructure of the sample implanted at 77°K differed from the others in that an amorphous surface layer was formed. No amorphous surface layer was observed in the sample implanted under the same conditions at room temperature.

Discussion:

The experimental results presented here indicate that decomposition of both Ni and Fe carbonyls results in the formation of a supersaturated fcc

in Fe-C[13] and Ni-C[5] alloys that were liquid quenched. Gas carburization of Ni produces Ni_3C identical to that observed here, however, gas carburization of Fe is reported to produce cementite only above 623° K while other carbides are formed at lower temperatures[14]. Again, ion implantation in Ni produced Ni_3C with crystal structure identical to that found here while Fe_2C has been reported to form after implantation of C into pure Fe[15]. Gas carburization allows for considerable atomic diffusion and the products formed have presumably approached thermodynamic equilibrium with the metastable phases observed present only due to sluggish kinetics. Liquid quenching and ion implantation do allow some atomic diffusion though very limited in comparison to carburization with the products presumably in a metastable equilibrium state. This study shows that even a severe quench from the gas phase fails to completely stop the system from approaching its equilibrium structure. This indicates that the carbides Ni_3C and Fe_3C are associated with a very high thermodynamic driving force for their formation even though both of these phases are metastable. The formation of an amorphous layer in the substrate held at low temperature indicates that although the saturated Ni-Ni_3C mixture is associated with a high thermodynamic driving force, a severe restriction of diffusion can result in the formation of an amorphous phase.

ACKNOWLEDGEMENTS

This work was carried out when one of the authors (SKM) was a Postdoctoral Fellow at the Los Alamos National Laboratory. SKM gratefully acknowledges the Director, Los Alamos National Laboratory, for granting the fellowship. We would like to thank R. Cordi for the Auger analysis and also acknowledge the support of the U. S. Department of Energy under contract W-7405-ENG-36.

REFERENCES

1. T. R. Jervis, J. Appl. Phys. 58 1400 (1985).
2. T. R. Jervis & L. R. Newkirk, J. Mat. Res. 1 420 (1986).
3. S. Nagakura, J. Phys. Soc. Jap. 12 482 (1957).
4. S. Nagakura, J. Phys. Soc. Jap. 13 1005 (1958).
5. S. R. Nishitani, K. N. Ishihara, R. O. Suzuki, & P. H. Singu, J. Mat. Sci. Lett. 4 872 (1985).
6. J. W. Edington, Electron Diffraction in the Electron Microscope, Monograph 2 in Practical Electron Microscopy in Materials Science, p. 110, Phillips, Eindhoven, (1975).
7. M. Hansen, Constitution of Binary Alloys, McGraw Hill, New York (1958).
8. H. Ohtani, M. Masebe, & T. Nishizawa, Trans. I. S. I. J. 24 857 (1984).
9. T. P. Ershova, D. S. Kamenetskaya, & L. P. Il'ina, Izv. Akad. Nauk. USSR, Met. 4 201 (1981).
10. R. C. Ruhl & M. Cohen, Scripta Metall. 1 73 (1967).
11. W. Stevens & A. G. Haynes, J. I. S. I. 183 349 (1956).
12. C. S. Roberts, Trans. AIME, 191 203 (1953).
13. F. H. Samuel, Zeit. Metallkde. 76 792 (1985).
14. S. Nagakura, J. Phys. Soc. Jap. 14 186 (1959).
15. D. M. Follstaedt & J. A. Knapp, "Binary & Ternary Amorphous Alloys of Ion Implanted Fe-Ti-C", To be Published in Mat. Res. Soc. Symp. Proc. 51.